



Graphite/Polyimide Composites Subjected to Biaxial Loads at Elevated Temperatures

Maciej S. Kumosa* and J. K. Sutter**

*Center for Advanced Materials and Structures
Department of Engineering, University of Denver
2390 S. York St., Denver Colorado
mkumosa@du.edu, tel: (303) 699-3236

** NASA Glenn Research Center at Lewis Field
21000 Brookpark Road, Cleveland, OH 44135





Abstract

- **First, we will review our most important research accomplishments from a five year study concerned with the prediction of mechanical properties of unidirectional and woven graphite/polyimide composites based on T650-35, M40J and M60J fibers embedded in either PMR-15 or PMR-II-50 polyimide resins.**
- **Then, an aging model recently developed for the composites aged in nitrogen will be proposed and experimentally verified on an eight harness satin (8HS) woven T650-35/PMR-15 composite aged in nitrogen at 315°C for up to 1500 hours.**
- **The study was supported jointly between 1999 and 2005 by the AFOSR, the NASA Glenn Research Center, and the National Science Foundation.**

We Were a Part of These Efforts!!!



Rocket Based Combined Cycle
Combustion Chamber Support Structure

NASA Glenn Announcement, March 2004.

“A lightweight high temperature polymer matrix composite (HTPMC) combustor support chamber for a Rocket Based Combined Cycle engine successfully survived hot-fire testing at ATK-GASL. This testing concludes a three year collaboration between NASA Glenn and Boeing to design, fabricate and test the support structure and fulfills a GPRR (Government Performance Reform Act) milestone for the UEEET (Ultra-efficient Engine Program). The support structure was prepared from a high temperature composite material, PMR-II-50”



Shear Testing of 8HS T650-35/PMR-15, 4HS M40J/PMR-II-50 and 4HS M60J/PMR-II-50

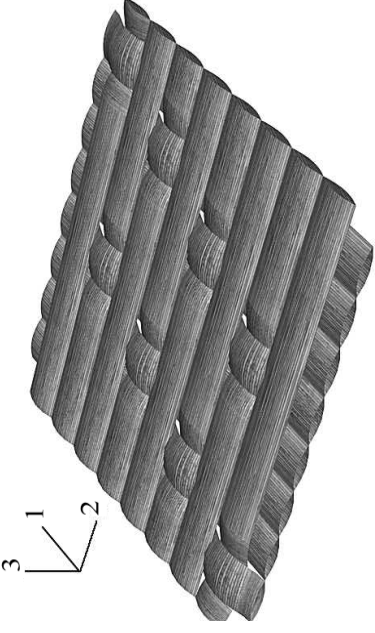
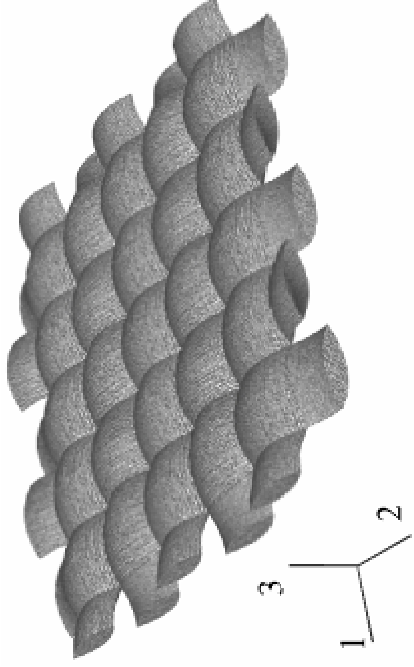
Mechanical behavior of unidirectional and woven graphite/polyimide composites based on medium (T650-35) and high (M40J and M60J) modulus graphite fibers with PMR-15 and PMR-II-50 polyimide resins tested under biaxial shear dominated stress conditions over a temperature range of 20°C to 316°C under dry and wet conditions has been investigated both experimentally and numerically.

M. Kumosa et al., Comparison of the 45° off Axis and Iosipescu Shear Tests for Woven Fabric Composite Materials, *Composites Technology & Research*, Vol. 24 (2002) pp. 3-16.

M. Gentz et al., Mechanical Behavior of a Woven Graphite/PMR-15 Composite at Room and Elevated Temperatures Determined from the ±45° Tensile and Iosipescu Shear Tests, *Journal of Composites Technology & Research*, Vol. 25, Issue 1 (2003) pp. 22-34.

M. Gentz, et al., In-Plane Shear Testing of Woven Graphite/Polyimide Composites with Medium and High Modulus Graphite Fibers at Room and 316°C Temperatures, *Composites Science and Technology*, Vol. 64 (2004) pp. 203-220.

Graphite/Polyimide Composites



Woven composite systems; plain (left) and eight harness satin 8HS (right)

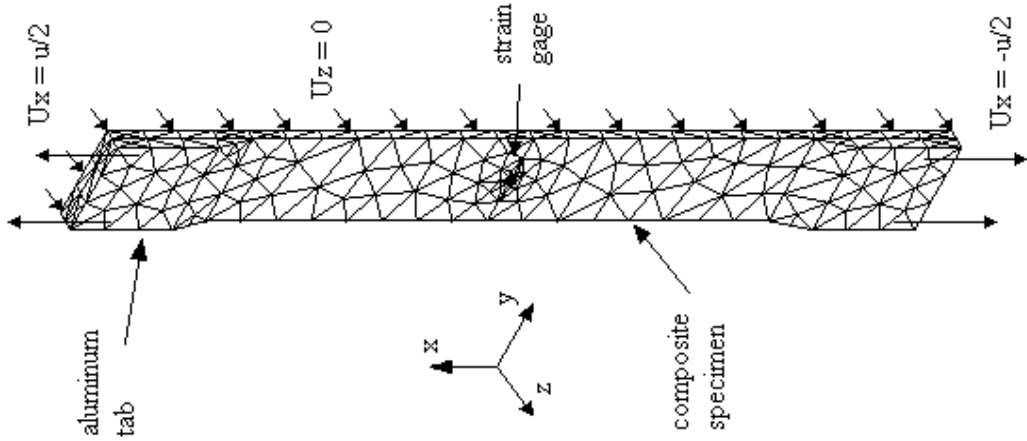
A major limitation of woven fiber/polymer matrix composite systems is the inability of these materials to resist intralaminar and interlaminar damage initiation and propagation under shear-dominated biaxial loading conditions.



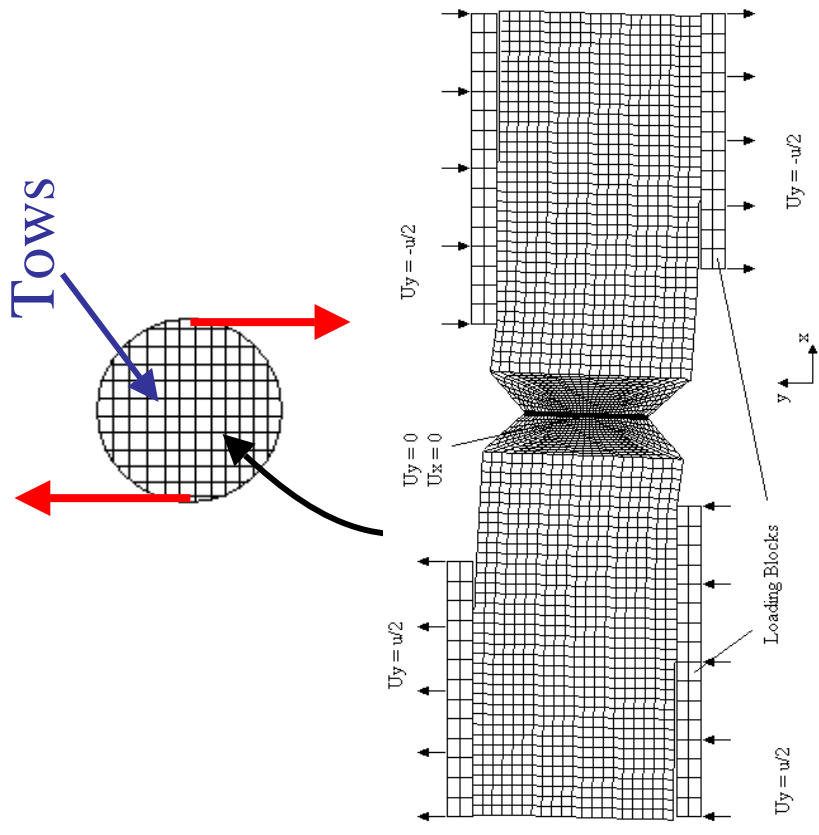
Biaxial Shear Dominated Strength of 8HS T650-35/PMR-15 System

- There are numerous shear test methods for woven fabric composites, each with its own advantages and disadvantages.
- Two techniques, which show much potential, are the **Iosipescu shear** and **$\pm 45^\circ$ tensile** tests. The application of these two tests for the shear testing of woven graphite/polyimide composites at room and elevated temperatures was evaluated in this project both experimentally and numerically.

Macroscopic FEM Models of $\pm 45^\circ$ Tensile and Iosipescu Shear Tests



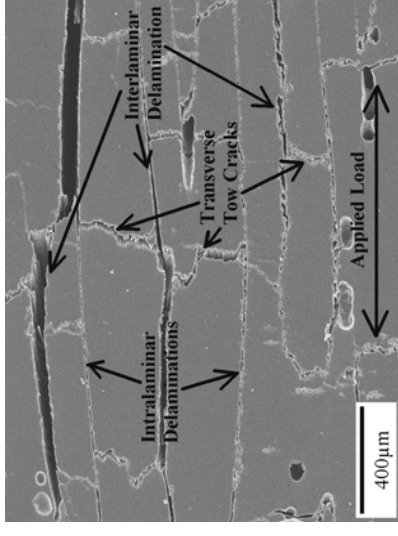
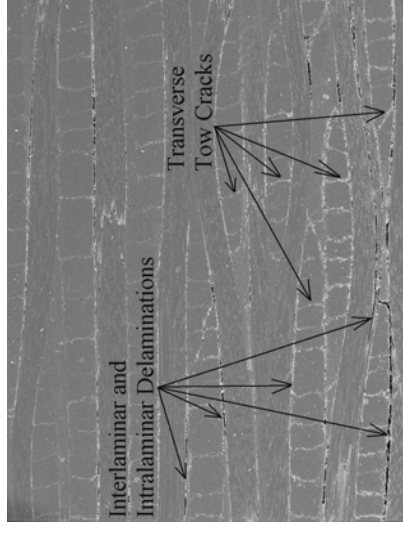
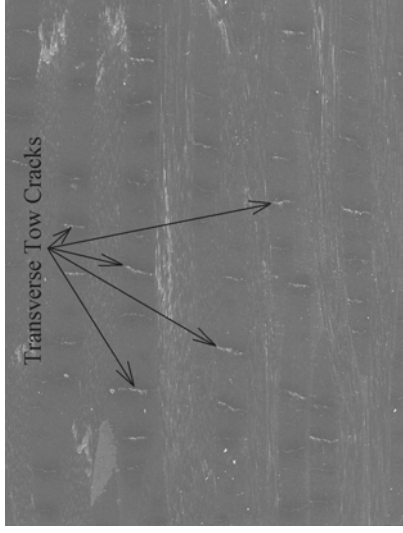
Finite element mesh of Iosipescu specimen.



Finite element mesh of Iosipescu specimen.

G. Odegard, K. Seetharam, and S. K. Kim, *Analysis of Woven Fabric-Reinforced Graphite/PMR-15 Composites under Shear-Dominated Biaxial Loads*, *Mechanics of Composite Materials and Structures*, Vol. 7 (2000) pp. 129-152.

SEM Analysis (Stages of Damage in 8HS T650-35/PMR-15)



Stages of crack initiation and propagation in 8HS T650-35/PMR-15 at room temperature under shear dominated in-plane loads.

G. Odegard, K. Searles and M. Kumosa, *Nonlinear Analysis of Woven Fabric-Reinforced Graphite/PMR-15 Composites under Shear-Dominated Biaxial Loads*, *Mechanics of Composite Materials and Structures*, Vol. 7 (2000) pp. 129-152.

M. Kumosa, G. Odegard, D. Armentrout, L. Kumosa, K. Searles and J. K. Sutter, *Comparison of the $\pm 45^\circ$ Off-Axis and Iosipescu Shear Tests for Woven Fabric Composite Materials*, *J. Composites Technology & Research*, Vol. 24, No. 1 (2002) pp.3-16.

M. Gentz, D. Armentrout, P. Rupnowski, L. Kumosa, J. K. Sutter and M. Kumosa, *Mechanical Behavior of a Woven Graphite/PMR-15 Composite at Room and Elevated Temperatures Determined from the $\pm 45^\circ$ Tensile and Iosipescu Shear Tests*, *Composites Technology & Research*, Vol. 25 (2003) pp. 22-34.

8HS T650-35/PMR-15; Iosipescu VS. $\pm 45^\circ$ Tensile Tests

Shear stresses at the onset of intralaminar damage and at the maximum loads from the $\pm 45^\circ$ and Iosipescu tests at room and 316°C temperatures for the 8HS T650-35/PMR-15 system.

T650/PMR-15	Shear Stresses at the Onset of Intralaminar Damage [MPa]		Shear Stresses at Maximum Loads [MPa]	
	$\pm 45^\circ$ (biaxial)	Iosipescu (shear)	$\pm 45^\circ$ (biaxial)	Iosipescu (shear)
at RT	56.6 \pm 2.0	94.8 \pm 1.3	82.0 \pm 0.15	105.8 \pm 2.6
at 315°C	37.3 \pm 5.2	59.9 \pm 1.2	50.8 \pm 6.0	71.8 \pm 4.2

G. Odegard, K. Searles and M. Kumosa, *Nonlinear Analysis of Woven Fabric-Reinforced Graphite/PMR-15 Composites under Shear-Dominated Biaxial Loads*, *Mechanics of Composite Materials and Structures*, Vol. 7 (2000) pp. 129-152..

M. Kumosa, G. Odegard, D. Armentrout, L. Kumosa, K. Searles and J. K. Sutter, Comparison of the $\pm 45^\circ$ Off-Axis and Iosipescu Shear Tests for Woven Fabric Composite Materials, *J. Composites Technology & Research*, Vol. 24, No. 1 (2002) pp.3-16.

M. Gentz, D. Armentrout, P. Rupnowski, L. Kumosa, J. K. Sutter and M. Kumosa, Mechanical Behavior of a Woven Graphite/PMR-15 Composite at Room and Elevated Temperatures Determined from the $\pm 45^\circ$ Tensile and Iosipescu Shear Tests, *Composites Technology & Research*, Vol. 25 (2003) pp. 22-34.



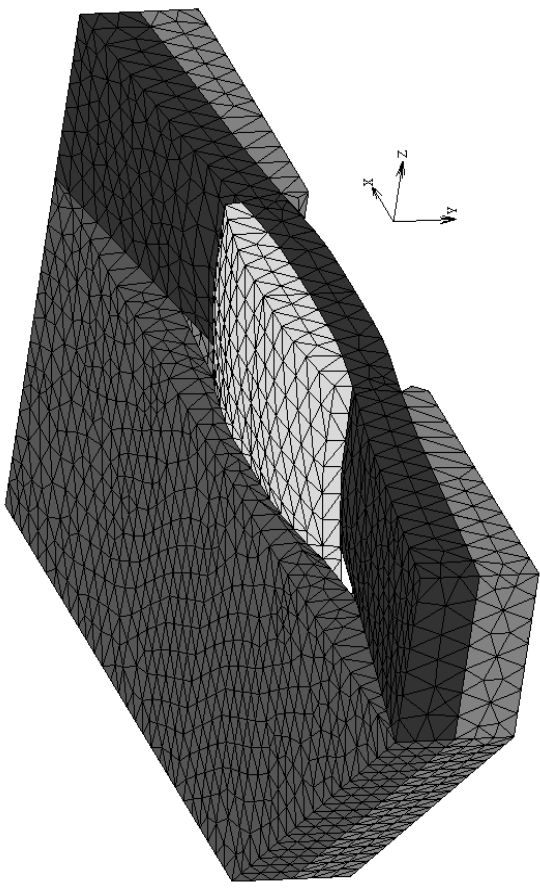
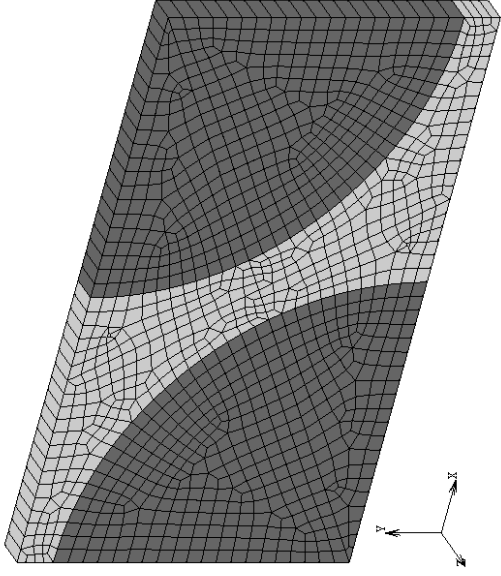
Visco-Elastic Meso- & Micro-Modeling of 8HS T650-35/PMR-15

To understand the effect of biaxial and shear dominated loads on the failure process of eight harness satin (8HS) T650-35/PMR-15, 3D models of the meso- and micro- unit cells were built. The magnitude of residual meso- and micro-stresses in the warp and fill tows and the stresses caused by purely mechanical shear and biaxial loads were numerically determined as a function of the cooling rate.

B. Benedikt, P. Rupnowski and M. Kumosa, Visco-Elastic Stress Distributions and Elastic Properties in Unidirectional Graphite/Polyimide Composites with Large Volume Fractions of Fibers, *Acta Materialia*, Vol. 51, No. 12 (2003) pp. 3483-3493.

P. Rupnowski and M. Kumosa, Meso- and Micro-Stress Analyses in an 8HS Graphite/Polyimide Woven Composite Subjected to Biaxial In-Plane Loads at Room Temperature, *Composites Science and Technology*, Vol. 63 (2003) pp. 785-799.

Visco-Elasto-Plastic Meso- Micro Modeling of 8HS T650-35/PMR-15



Finite element representations of unidirectional (left) and 8HS woven (right) graphite/polyimide composites for visco-elasto-plastic micro- and meso-stress analyses.

P. Rupnowski, M. Gentz and M. Kumosa, Mechanical Response of a Woven Graphite/Polyimide Composite to In-Plane Shear Dominated Biaxial Loads at Room and Elevated Temperatures, *Acta Materialia*, Vol. 52, No. 19 (2004) pp. 5603-5613.

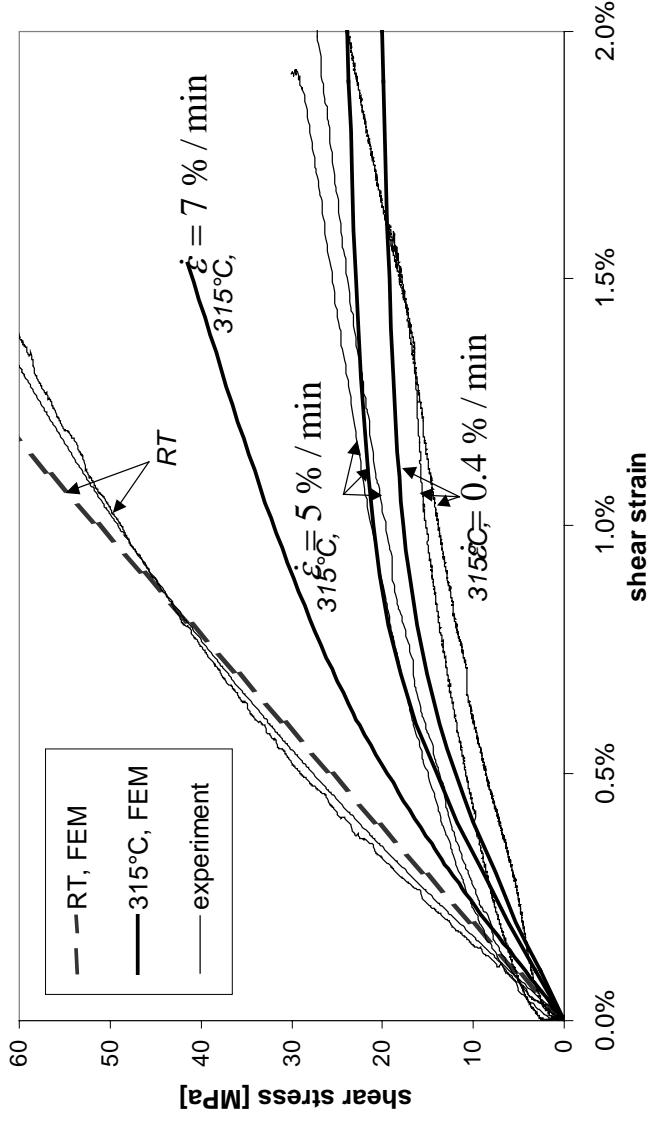
Meso- & Micro- Stress Distributions in 8HS T650-35/PMR-15

Meso- and micro-stresses in the center of the tow in the undulation region of 8HS T650/PMR-15 for various external in-plane loads at room temperature.

Load case	Meso-Stresses [MPa]						Micro-Stresses [MPa]
	σ_{xx} (trans. in-plane)	σ_{yy} (longi. in-plane)	σ_{zz} (trans. out of plane)	σ_{xz} (in-plane shear)	Failure Index Tsai-Hill	σ_1 (max. principal stress in the matrix)	
Case 1 (ΔT only) on cooling	64	-119	18	-1	0.6	94	
Case 2 (ΔT +TX)	79	-129	16	-1	1.1	107	
Case 3 (ΔT +TZ)	68	145	20	-1	0.7	102	
Case 4 (ΔT +S) Iosipescu	66	-98	19	108	3.9	208	
Case 5 (ΔT +TX+TZ)	83	136	17	0	1.2	111	
Case 6 (ΔT +TX+S)	81	-107	17	109	4.4	222	
Case 7 (ΔT +TZ+S)	70	167	20	109	4.0	216	
Case 8 (ΔT +TX+TZ+S) +/- 45 deg test	85	158	18	110	4.6	230	

ΔT residual stresses, TX(Z) applied in-plane tensions along the warp and fill tows, S in-plane shear with TX= TZ =S=100MPa

Visco-Elasto-Plastic Meso- Micro Modeling of 8HS T650-35/PMR-15



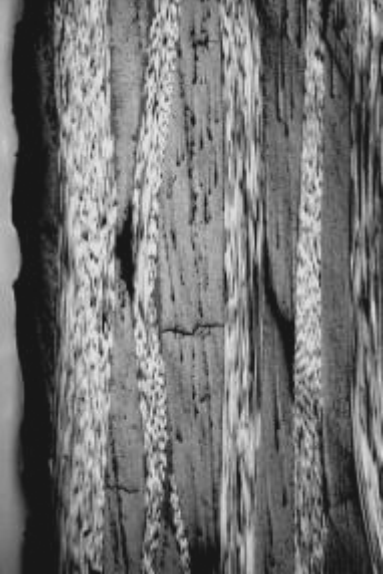
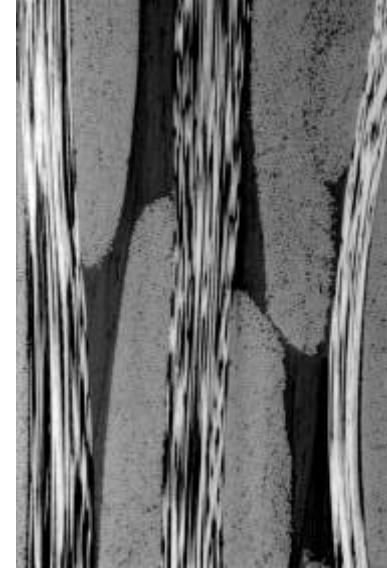
The macro-response of the composite to shear could be accurately predicted as a function of temperature and in-plane shear loads if the actual composite architecture as well as the fiber and matrix properties are considered.



Critical Issues

- The weakest fracture mode in the 8HS T650/PMR-15 composite is the combined state of stress consisting of in-plane shear and biaxial tension along the warp and fill tows. In shear (Iosipescu test), transverse tow cracks initiate at approximately 95 MPa shear stress. Under biaxial shear dominated loads ($\pm 45^\circ$ off-axis), the tow cracks initiate at 57 MPa shear stress. This can be explained numerically.
- Linear elastic macro- and micro- stress analyses cannot explain the very complex fracture/failure process in woven graphite/polyimide laminates subjected to in plane shear dominated loads. Also, non-linear macro-approaches are not suitable to explain the effect of biaxial loads and residual stresses on the damage initiation stresses.
- Visco-elasto-plastic analytical and FEM stress analyses are needed. In particular, the effect of manufacturing residual stresses on the failure process must be considered.
- The type of fracture and the critical loads will be affected by physical and chemical aging.

Residual Stresses and Tow Micro-Cracking



Cross-sections of woven 8HS T650-35/PMR-15 (left), 4HS M40J/PMR-II-50 (middle) and 4HS M60J/PMR-II-50 (right) composites after manufacturing and post curing

- Residual stresses in graphite/polyimide composites depend primarily on:
 - Visco-elasto-plastic stiffness properties and CTEs of polyimide resins
 - Fiber elastic properties (longitudinal, transverse, shear)
 - CTEs of fibers (both longitudinal and transverse)
 - Manufacturing conditions
 - Aging conditions
 - Fiber/matrix interfaces
 - Composite architecture,
 - etc., etc., etc.



An Evaluation of Elastic Properties and Coefficients of Thermal Expansion of Graphite Fibers

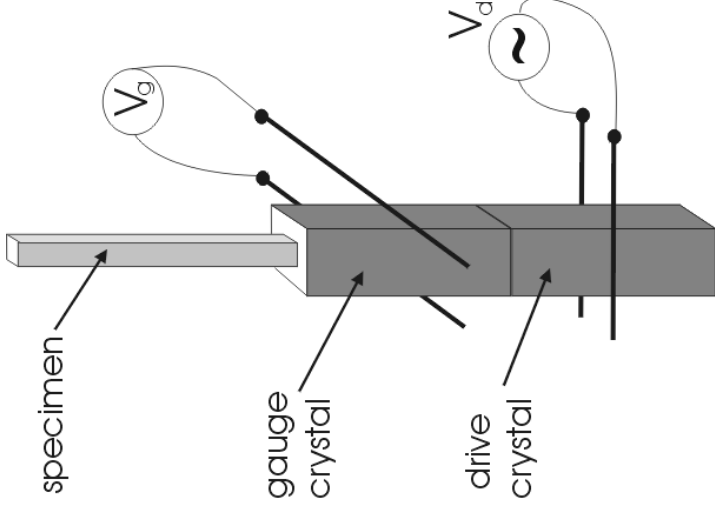
A methodology has been suggested for the evaluation of stiffness properties (longitudinal, transverse and shear) and coefficients of thermal expansion (both longitudinal and transverse) of medium (T650-35) and high (M40J and M60J) modulus graphite fibers. The methodology was subsequently used to determine the stiffness and thermal properties of the fibers from the macroscopic input data of unidirectional and woven composites based on the same fibers embedded either in PMR-15 or PMR-II-50 polyimide resins.

P. Rupnowski, M. Gentz, J.K. Sutter and M. Kumosa, An Evaluation of Elastic Properties and Coefficients of Thermal Expansion of Graphite Fibers from Macroscopic Composite Input Data, *Proceedings of the Royal Society*, Vol. 461 (2005) pp. 347-369.

P. Rupnowski, M. Gentz, J. K. Sutter and M. Kumosa, An Evaluation of the Elastic Properties and Thermal Expansion Coefficients of Medium and High Modulus Graphite Fibers, *Composites Part A: Applied Science and Manufacturing*, Vol. 36 (2004) pp. 327-338.

T650-35, M40J, M60J, M60J; Elastic Properties

The room temperature properties of the T650-35, M40J and M60J fiber systems were measured using the three-component oscillator resonance method. The macro-coefficients of thermal expansion of the composites and their neat resins were obtained by length dilatometry. Then, the fiber properties were calculated (re-calculated for T650-35).



$$E \text{ or } G = \rho \left(\frac{f_{\text{spec}} L}{n} \right)^2$$

Eshelby/Mori-Tanaka Approach

$$C_f = \left[\left(\frac{1}{f_v} - 1 \right) C_m (I - S) (C_m^{-1} - C_c^{-1}) + I \right] \left[C_m^{-1} - (S - f_v (S - I)) (C_m^{-1} - C_c^{-1}) \right]^{-1} \frac{1}{f_v}$$

$$\alpha_f = \frac{1}{f_v} C_f^{-1} \left[(C_m - C_f) (S - f_v (S - I)) - C_m \right] (\alpha_m - \alpha_c) + \alpha_m$$

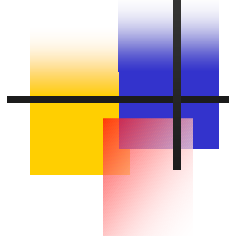
where

C_f , C_c , C_m are the stiffness matrices of the fibers, composite and resin, respectively

S is the Eshelby tensor and I is the identity matrix

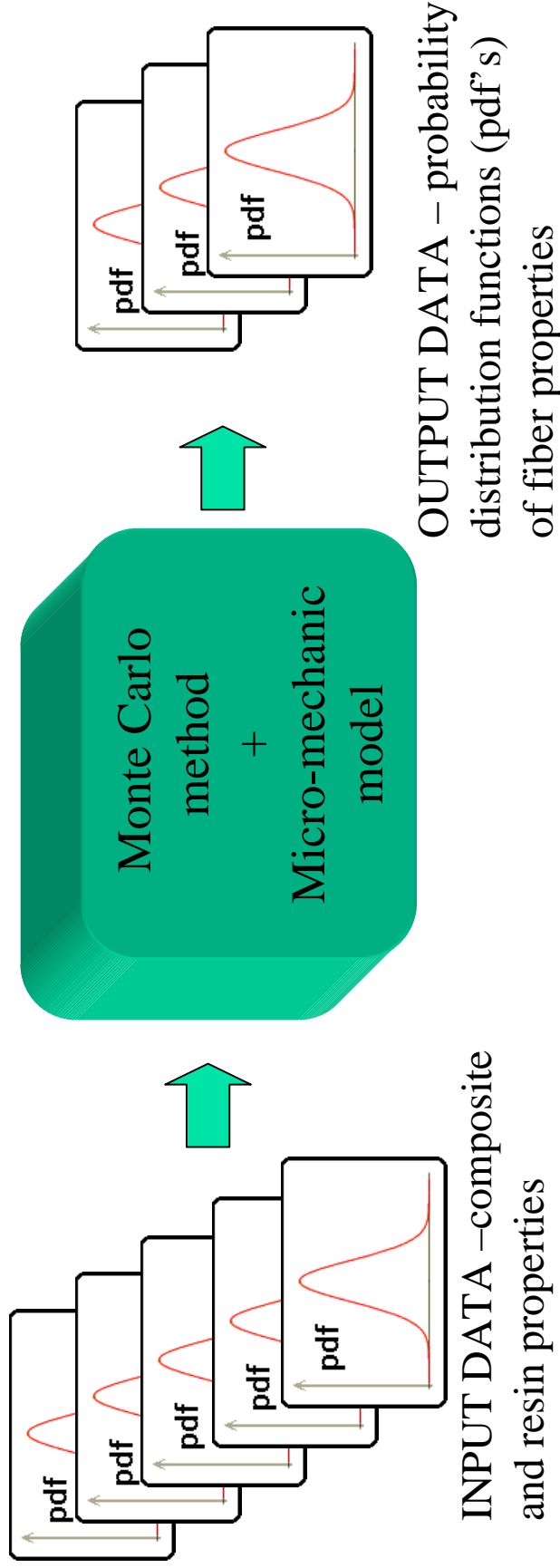
α_f , α_m , and α_c are the column vectors of the CTEs for the fibers, matrix and composite, respectively

f_v is the volume fraction of fibers



Macro- to Micro-Approach

Classical error analysis based on the Monte Carlo method applied to the inverse Eshelby/Tanaka-Mori model was employed to compute the uncertainty of indirect evaluation of graphite fiber properties.



T650-35, M40J, M60J; “Final” Estimates

	E_{f11} [GPa]	E_{f22} [GPa]	G_{f12} [GPa]	G_{f23} [GPa]	ν_{f12}	CTE (long.) $10^{-6}/K$	CTE (trans.) $10^{-6}/K$
T650-35	224 ± 3 (243)	15.4 ± 0.5 (13.8)	21.1 ± 1.1 (23.1)	5.8 ± 0.4 (5.0)	0.44 ± 0.02 (0.29)	-1.16 ± 0.05 (-0.84)	13.3 ± 0.8 (7.8)
M40J	325 ± 19 (377)	10.8 ± 0.3	20.8 ± 2	3.9 ± 0.1	0.22 ± 0.05	-2.0 ± 0.1 (-0.83)	8.7 ± 1.6
M60J	500 ± 2 (588)	9.4 ± 0.5	-	-	-	-2.0 ± 0.2 (-1.1)	18.0 ± 4

() from literature



Macro- to Micro-Approach; Limitations

- The newly developed experimental/numerical methodology is extremely sensitive to the accuracy of the input macro-data, especially in the case of the elastic properties.
- However, using the macro composite input data from the oscillator resonance method and length dilatometry in conjunction with EMT and FEM, high quality estimates of fiber properties were obtained.
- The methodology also works very well with thermal expansions of graphite fibers.



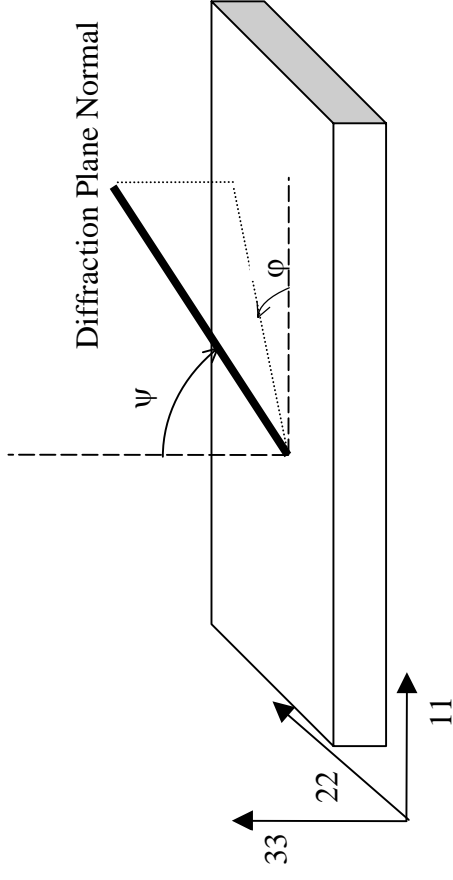
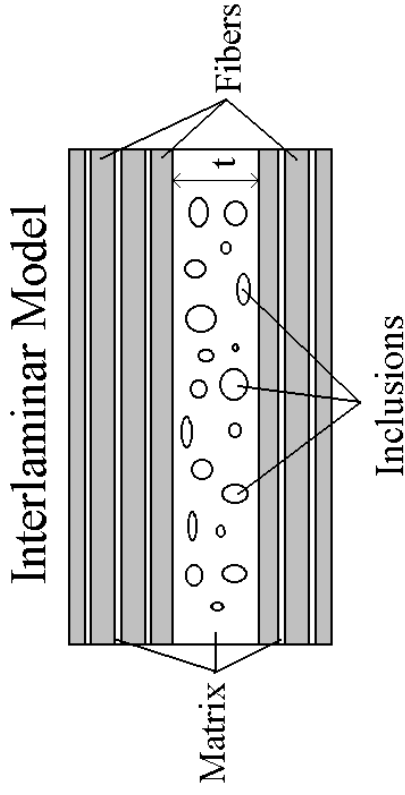
X-Ray Diffraction Tests on T650-35/PMR-15 Composites with Embedded Inclusions

Interlaminar residual thermal stresses in unidirectional and woven (8HS) T650-35/PMR-15 composites were determined both experimentally and numerically as a function of the manufacturing process. Numerous XRD measurements were made to determine residual strains and stresses in embedded Al and Ag inclusions placed in four ply 8HS woven and 6 ply unidirectional graphite/PMR-15 composites.

B. Benedikt, M. Kumosa, P.K. Predecki, L. Kumosa, M.G. Castelli and J.K. Sutter, *An Analysis of Residual Thermal Stresses in a Unidirectional Graphite/PMR-15 Composite Based on the X-ray Diffraction Measurements, Composites Science and Technology*, Vol. 61, No. 14 (2001) pp. 1977-1994.

B. Benedikt, P. Rupnowski, L. Kumosa, J. K. Sutter, P.K. Predecki and M. Kumosa, *Determination of Interlaminar Residual Thermal Stresses in a Woven 8HS Graphite/PMR-15 Composite Using X-Ray Diffraction Measurements, Mechanics of Advanced Materials and Structures*, Vol. 9 (2002) pp. 1-20.

X-Ray Diffraction Tests on T650-35/PMR-15 Composites with Embedded Inclusions

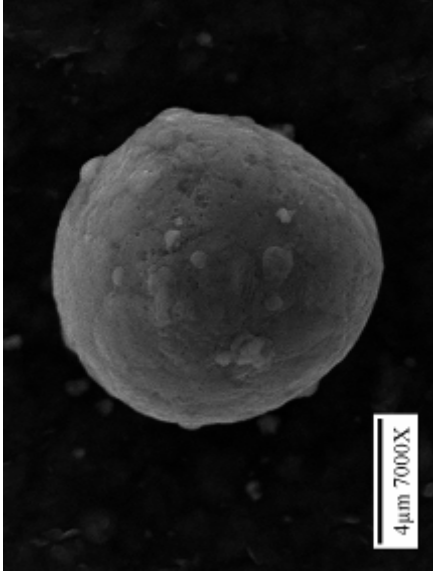


$$\varepsilon_{\phi\psi} = \frac{d_{\phi\psi} - d_0}{d_0} = \varepsilon_{11} \cos^2 \phi \sin^2 \psi + \varepsilon_{12} \sin 2\phi \sin^2 \psi +$$

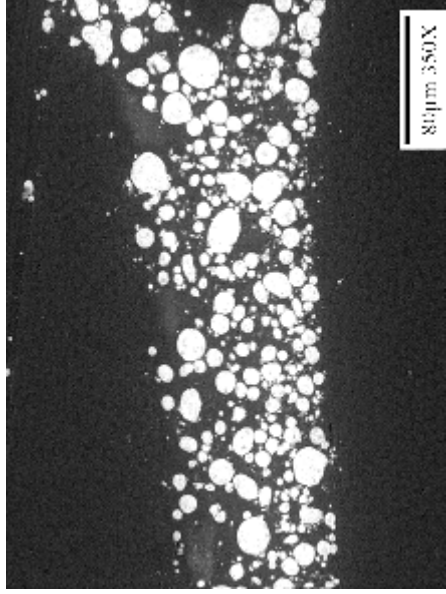
$$\varepsilon_{22} \sin^2 \phi \sin^2 \psi + \varepsilon_{33} \cos^2 \psi + \varepsilon_{13} \cos \phi \sin 2\psi + \varepsilon_{23} \sin \phi \sin 2\psi$$

Lattice spacing in unstressed (d_0) and stressed ($d_{\phi\psi}$) particles measured by XRD.

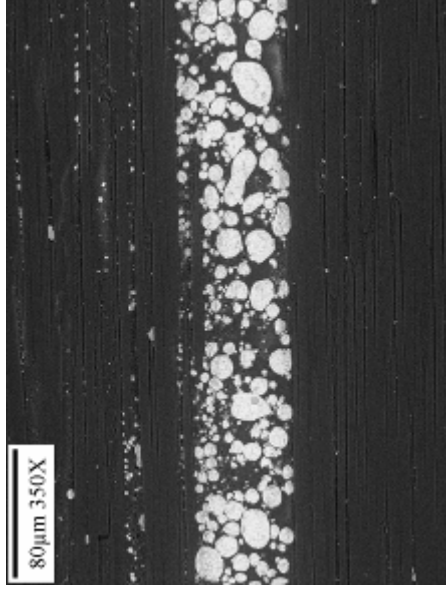
X-Ray Diffraction Tests on T650-35/PMR-15 Composites with Embedded Inclusions



Aluminum inclusion



Embedded Al inclusions between woven plies



Embedded Al inclusions between unidirectional plies

Interlaminar Residual Stresses in 8HS T650-35/PMR-15 Composite

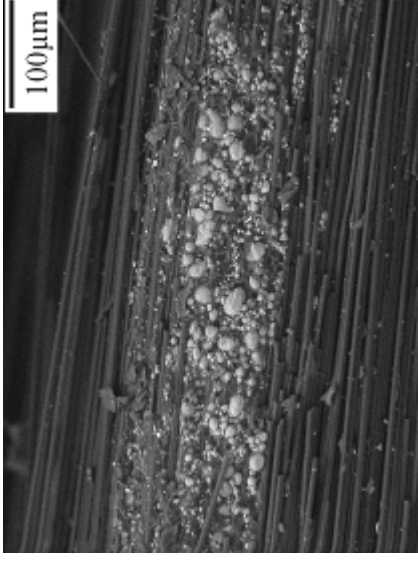
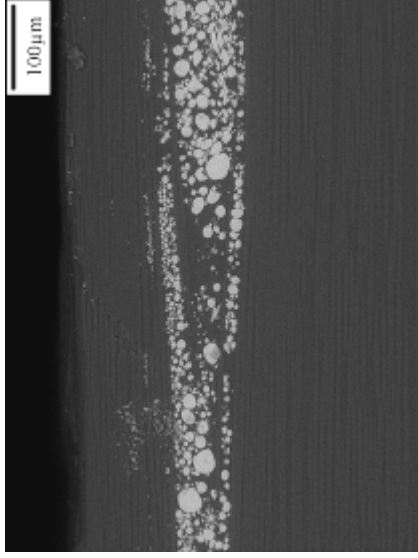
- Residual stresses in unidirectional and 8HS T650-35/PMR-15 composites were determined
 - just on cooling (no external loads applied)
 - with external bending loads (small and large)
 - after aging in N₂ and air

	X-ray with Eshelby/Mori-Tanaka			Plate theory		
	σ_{11} [MPa]	σ_{22} [MPa]	σ_{33} [MPa]	σ_{11} [MPa]	σ_{22} [MPa]	σ_{33} [MPa]
Linear elastic	70.7 ± 17	71.1 ± 17	36.7 ± 16	94.0	94.0	0
Visco-elastic	67.3 ± 17	67.6 ± 16	33.0 ± 16	63.1	63.1	0

Residual interlaminar stresses in 8HS T650-35/PMR-15 (no external loads and no aging)

X-Ray Diffraction Experiments on Graphite Fiber/Polyimide Composites Subjected to Aging

(XRD) measurements of residual strains in embedded aluminum spherical inclusions were performed to evaluate the residual interlaminar stresses in unidirectional and woven 8HS T650/PMR-15 composites subjected to aging either in air or nitrogen and external bending loads.



Unidirectional T650-35/PMR-15 system aged in nitrogen (left) and in air (right) for 1170 hours.

- B. Benedikt et al. Determination of Interlaminar Residual Stresses in a Woven 8HS Graphite/PMR-15 Composite Using X-ray Diffraction Measurements, *Mechanics of Advanced Materials and Structures*, Vol. 9 (2002) pp. 375.
- B. Benedikt et al., Analysis of Stresses in Aluminum Particles Embedded Inside Unidirectional and Woven Graphite/Polyimide Composites Subjected to Large Bending Loads, *Mechanics of Advanced Materials and Structures*, Vol. 11, No. 1 (2004) pp. 31-49.
- B. Benedikt et al., X-Ray Diffraction Experiments on Aged Graphite Fiber/Polyimide Composites with Embedded Aluminum Inclusions, *Composites Part A*, Vol. 35 (2004) pp. 667-681.



Our New Model of Aging in Nitrogen

Based on:

“The Mechanical Response of Eight Harness Satin (8HS) Woven T650-35/PMR-15 Aged in Nitrogen”

by:

P. Rupnowski, M. Gentz, D. Armentrout, J. K. Sutter and , M. Kumosa

published in:

Acta Materialia, Vol. 53, No. 17 (2005) pp. 4555-4565.

Our model has not yet been presented to this community.



The Mechanical Response of Eight Harness Satin (8HS) Woven T650-35/PMR-15 Aged in Nitrogen

- The mechanical response of an eight harness satin woven T650-35/PMR-15 composite to aging in nitrogen at 315°C for up to approximately 1500 hours was investigated both experimentally and numerically.
- The aging stresses in the composite were numerically predicted on a meso-scale using the concept of a unit cell.

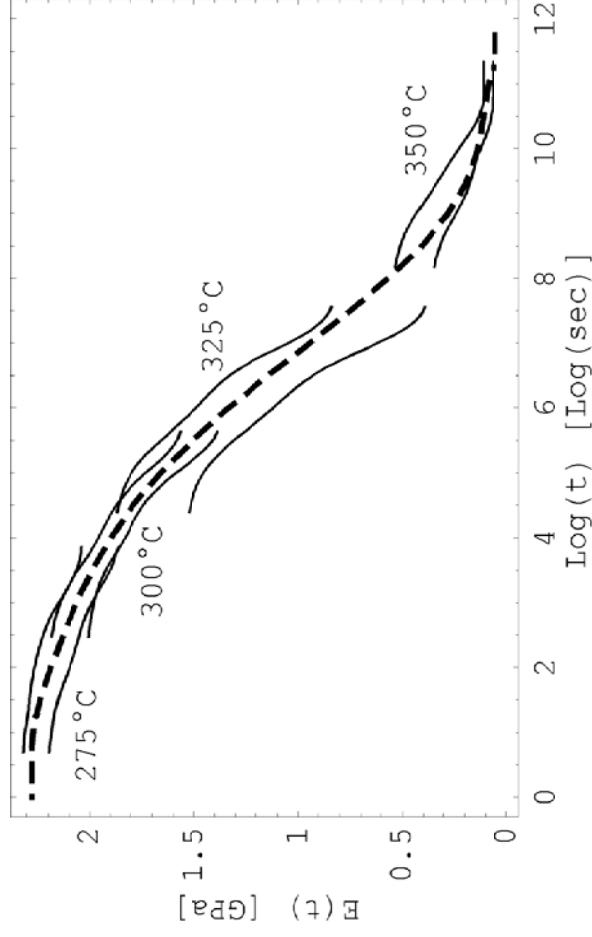
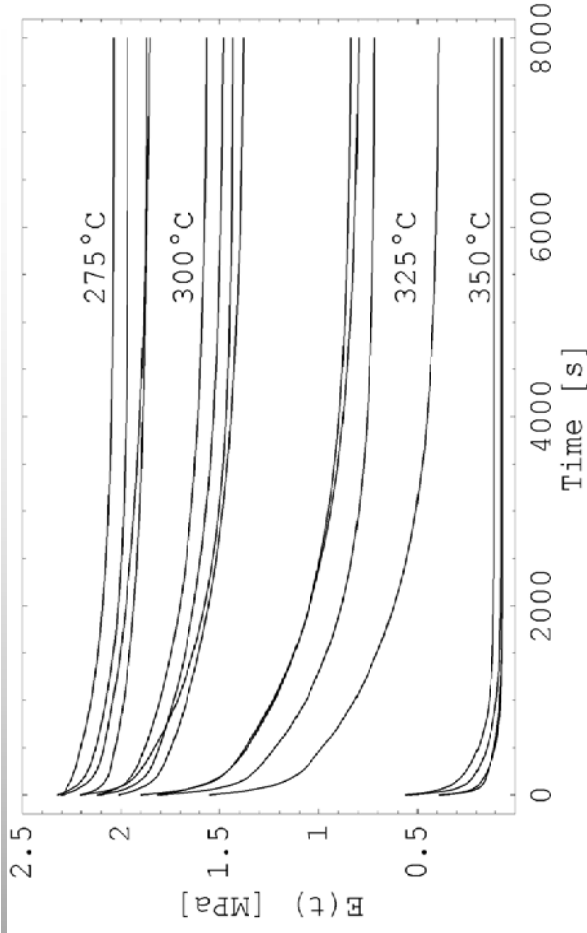


The Mechanical Response of Eight Harness Satin (8HS) Woven T650-35/PMR-15 Aged in Nitrogen

- **Viscoelastic, age stiffening, and volumetric shrinkage effects were considered in the simulations to describe the mechanical behavior of the neat PMR-15 polyimide in the composite subjected to aging at 315°C.**
- **To verify the numerical predictions, the strength and stiffness of the composite were measured as a function of aging time using the $\pm 45^\circ$ tensile test.**

Viscoelastic Properties of PMR-15

A series of mechanical 2 h long relaxation tests at 275, 300, 325 and 350°C were performed under constant displacement to obtain stresses and strains as a function of time ($\sigma(t)$ and $\varepsilon(t)$). Then, an optimization technique was employed to determine the relaxation modulus $E(t)$ for each test (**upper right**). Subsequently, a master curve was constructed (**lower right**) and the horizontal thermal shift factors were obtained.



Age Stiffening & Shrinkage of PMR-15

- When a polymer is physically aged its viscoelastic response changes as a function of aging time. Typically, the relaxation process slows down with aging. This age stiffening effect in PMR-15 can be modeled by shifting the time scale in its viscoelastic model. Consequently,

$$\sigma_{ij}(t) = \int_0^t C_{ijkl} (\psi(t) - \psi(\tau)) \cdot d\varepsilon_{kl}(\tau)$$

where

$$\psi(t) = \int_0^t a_h(\tau) d\tau$$

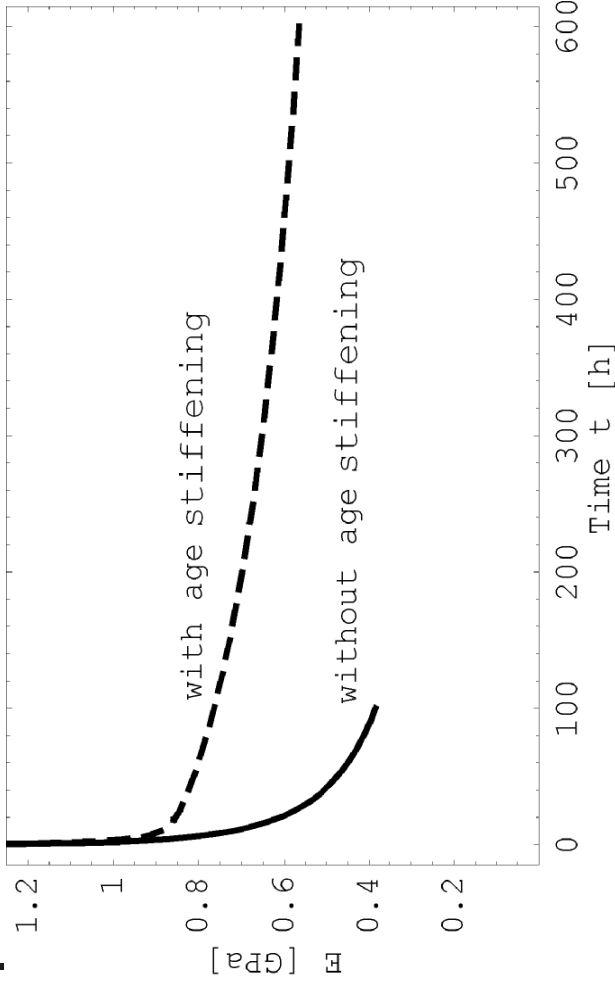


Age Stiffening & Shrinkage of PMR-15

a_h in the previous constitutive equation is a **horizontal aging shift factor** taken from [Kamvouris, J. E., Roberts, G. D., Pereira, J.M., and Rabzak, C., (1997), "Physical and Chemical Aging Effects in PMR-15 Neat Resin", *ASTM STP 1302*, pp. 243-258.]

- The aging shrinkage strain rate for PMR-15 was determined for times ranging from 0 to 300 h and was found to be $-23.4 \cdot 10^{-6}/h$. The same rate was assumed in the aging simulations of the composite for up to 1000h.

Viscoelastic Properties of PMR-15



Long term relaxation
curve with and
without age
stiffening (left)

- Age stiffening strongly affects the shape of the relaxation functions in the considered time range and therefore cannot be neglected in the computations of stresses in the aged composite.
- An aging model without age stiffening would underestimate the aging stresses in the composite approximately by a factor of two.



Aging Experiments

- Twenty-two specimens with the fibers aligned at $\pm 45^\circ$ from their long axis were waterjet cut from a composite panel. The dimensions of the specimens were 153.5 x 25.4 x 5.34 mm. Following waterjet cutting the specimens were dried in a vacuum at 110°C for 24 h.
- The specimens were placed in an oven in a static nitrogen atmosphere at room temperature. The temperature of the oven was ramped at 5°C per minute until 315°C was reached.
- Once the isothermal aging temperature was achieved, the aging time started. From the twenty specimens four specimens each were aged at 288, 624, 958, 1296, and 1535 h.



Aging Experiments

- **The $\pm 45^\circ$ tensile tests were performed at room temperature at a rate of 1 mm/min. until failure.**
- **Two room temperature tensile tests at 0 aging time were performed and a minimum of three room temperature tensile tests at all other aging times was performed.**
- **During the $\pm 45^\circ$ tests, acoustic emission (AE) was monitored by a D9215 sensor from Physical Acoustic Corp. (PAC)**



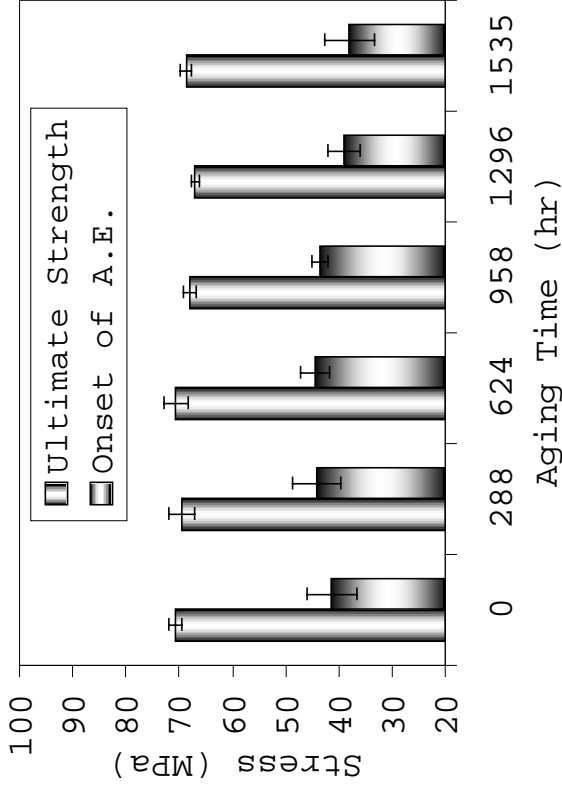
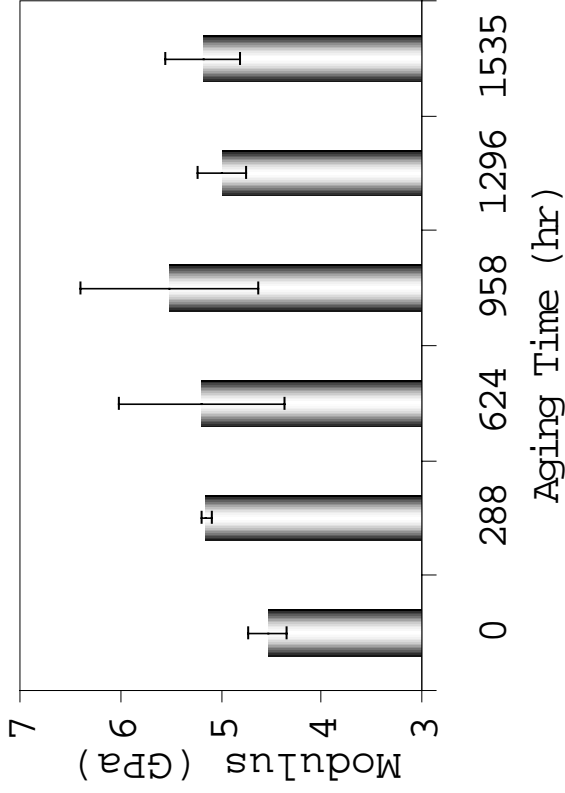
Aging Experiments

- Results from the $\pm 45^\circ$ experiments on the aged composite specimens included:
 - (1) the **ultimate strength** of the $\pm 45^\circ$ specimens,
 - (2) stress at the **initiation of intralaminar damage** as determined by AE,
 - (3) the **shear modulus**

All as a function of aging time at 315°C .



Aging Experiments



- Between 0 and 288 h of aging time the modulus increased approximately 12%. Then, the modulus was unchanged within the variability of the measurements.
- The ultimate shear strength was unchanged as a function of aging.
- Aging did not affect noticeably the onset of intralaminar damage.

Modeling

The Eshelby/Mori-Tanaka model was employed to obtain the viscoelastic properties and shrinkage of the tows. Then, the properties of the tows were introduced into a meso unit-cell representing the composite (see right). Subsequently, aging was simulated using the unit-cell and the meso- stresses and strains in the composite were determined as a function of time.

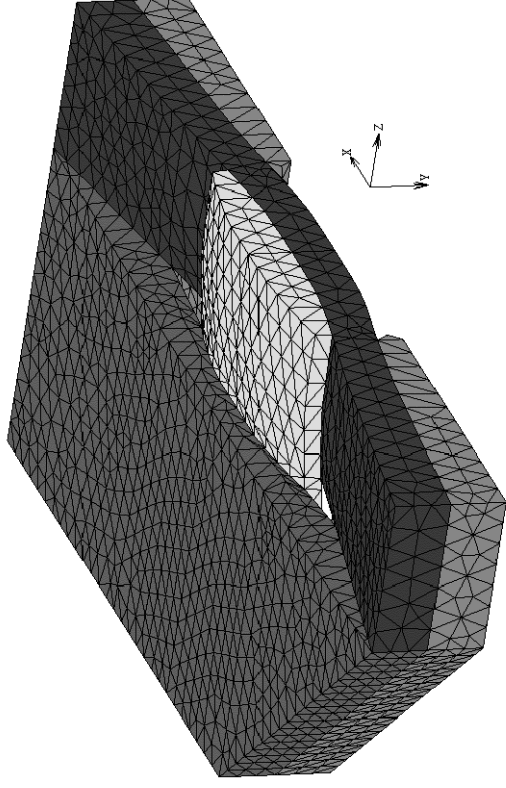
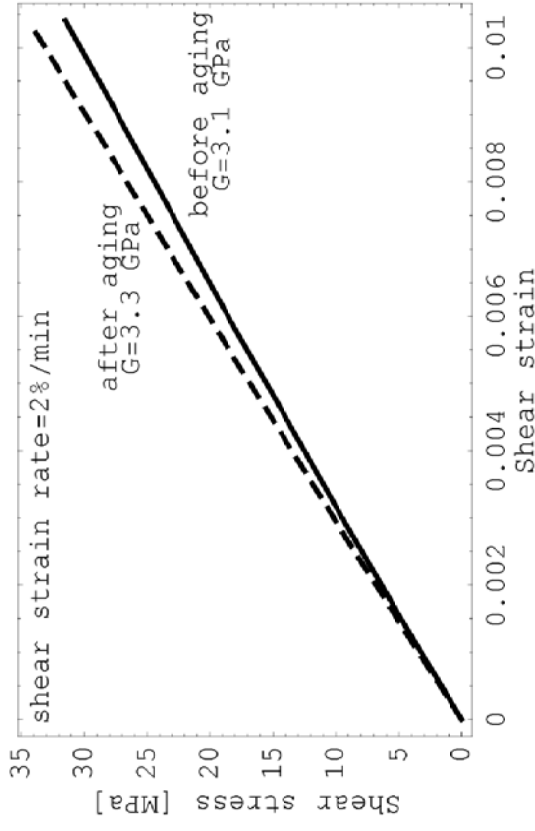
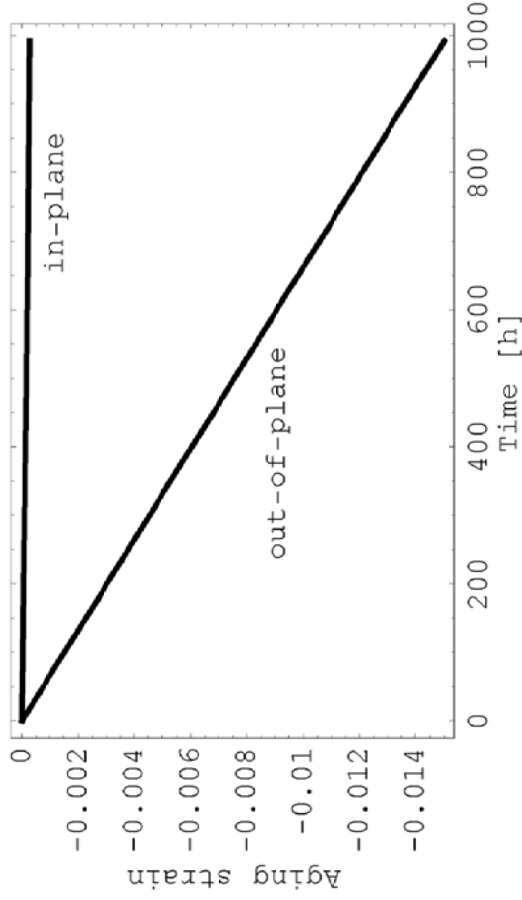


Figure 1

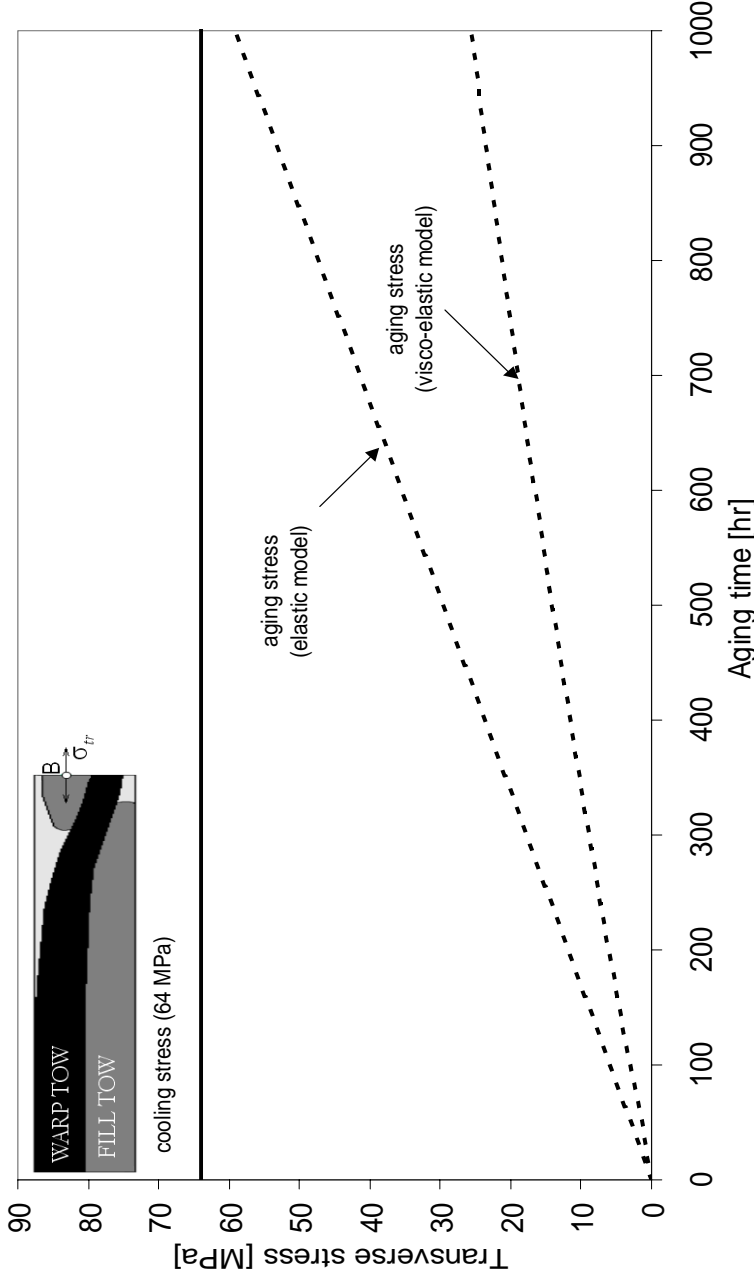
Modeling Results



Numerical in- and out-of-plane shrinkage strains (*) as a function of aging at 315°C
***) not yet experimentally verified).**

Shear stress vs. shear strain diagrams and the shear moduli at 315°C before and after aging for 1000 hours.

Modeling Results



The maximum transverse stress in the tows (**above**) after aging for 1000 hours at 315°C, as determined from the model, was approximately 85 MPa (**upper limit, could be even lower!**).

After cooling without aging the stress is appr. 64 MPa.



Conclusions

- Aging in nitrogen at 315°C for up to 1500 hours had a very small effect on the strength, onset of intralaminar damage, and the shear modulus of 8HS T650-35/PMR-15.
- The stress relaxation in PMR-15 that takes place at elevated temperature substantially reduces aging stresses in the composite.
- The aging stresses inside the tows were much smaller than the cooling stresses after the manufacturing cycle.
- Our numerical predictions agreed well with the experimental results.